The Sun's five-minute oscillations observed with an amateur spectroheliograph

Cédric Champeau

Working draft, 16 September 2026

Abstract. The surface of the Sun vibrates: it rises and falls with a period close to five minutes. We show here that these vibrations can be measured from the ground with an amateur spectroheliograph and a 102 mm refractor. On 15 September 2026, 336 scans of the solar disc were recorded over six hours in a line of iron. The JSol'Ex software reconstructs the images and measures, at every point of the surface, the velocity of the material along the line of sight. By sorting these motions according to their rhythm and their size, we obtain a diagram in which the power is concentrated along narrow lines: each one corresponds to a family of vibrations, and this is the expected signature of sound waves trapped beneath the surface. Six of these lines are separated, and their frequencies are compatible with those measured from space by the SOHO satellite. This detection and identification do not depend on any instrumental correction. An imperfection in the mount's tracking, which slightly shifts the content of the images, is then measured and corrected: the lines become sharper, while their frequencies do not change. An additional band appears near the position expected for another family of waves, called the f mode, but its position does not match the published measurements; its nature remains to be established.

1 Introduction

In 1962, Leighton, Noyes and Simon [1] discovered that the surface of the Sun oscillates, with a period of about five minutes. They measured this motion through the Doppler effect: when a region of the surface moves towards us, the light it emits is slightly shifted towards blue, and towards red when it moves away.

Ulrich [2] explained these oscillations: they are sound waves, trapped in the layers beneath the surface, which resonate like sound in a musical instrument. An important consequence of this explanation is that not every combination of rhythm and size is possible. Only some are, just as an organ pipe produces only certain notes. If the motions of the surface are sorted according to their rhythm, that is their frequency, and according to their size, that is the distance between two crests of the wave, the power is therefore not distributed at random: it is concentrated along narrow lines, called ridges. Each ridge corresponds to a family of waves that probe the interior of the Sun at different characteristic depths.

Deubner [3] observed these lines for the first time in 1975. He could distinguish three or four of them. Space observations then went much further, with the SOHO satellite [4], and later with Hinode [5].

From the ground, turbulence in the Earth's atmosphere blurs fine details and limits what can be seen [6]. Amateur spectroheliographs, derived from the Sol'Ex, record the complete shape of a line of the solar spectrum at every point of the disc, with a quality recognised by professional observatories [7]. They therefore give access to the velocity of the material at every point. The question asked here is simple: can such an instrument, on an amateur mount and under an ordinary sky, recover Deubner's ridges and identify them by comparison with space measurements?

Two quantities are enough to read the diagram. The first is the **frequency**, expressed in millihertz: 3 mHz corresponds to one oscillation every 333 seconds, a little more than five minutes. The second is the **degree**, written ℓ: it is the harmonic degree, which characterises the size of the structures at the surface: the higher it is, the smaller the waves. At degree 800, a complete wave measures about 5,500 km, that is 2,700 km from a crest to the neighbouring trough, to be compared with the solar radius of 696,000 km. This correspondence between size and degree is that of Gizon and Birch [8].

2 Instrument and observations

2.1 Instrument

Table 1: Instrument.

Item	Characteristic
Refractor	SVBony SV48P, 102 mm, 663 mm focal length
Spectroheliograph	MLAstro SHG 700, 7 μm slit
Camera	G3M678M, 1×1 binning
Mount	MLAstro SAL-33, with harmonic drives
Size of a pixel on the Sun	0.69 arcsecond, i.e. 503 km at disc centre
Dispersion	one pixel of the spectrum corresponds to a velocity of 5,737 m/s

The line chosen is that of neutral iron at 5434.5 Å. Its effective Landé factor is very small, which makes it only weakly sensitive to magnetic fields under ordinary photospheric conditions and limits the risk of mistaking a magnetic effect for a motion; Zeeman effects nevertheless remain measurable in the strongest fields, at the core of sunspots [9]. It has already been used to study waves at the solar surface [10]. It is wide enough to be sampled by more than three pixels of the spectrum, which is necessary to measure its position accurately.

2.2 Observations

Three sessions were recorded, on 13, 14 and 15 September 2026: 270, 154 and 336 retained scans, over durations of 4.5 h, 2.4 h and 6.0 h. The longer a session, the better neighbouring frequencies can be told apart: the resolution thus improves from 114 microhertz on 14 September to 46 on the 15th. A preliminary session, on 12 September, had served to develop the protocol; it is not used here. Everything that follows is based on the 15 September session alone, the most complete and the best resolved; the other two serve only as a check, to verify that the same ridges are found in them.

That session took place on 15 September 2026, from 07:49 to 13:49 UTC, at Montaigu-Vendée, France. Each scan of the disc is recorded in a separate video file, whose header provides the exact time. Eighteen scans out of 354 were discarded after visual inspection of the reconstructed images, because they showed an obvious defect: wrong geometry, artefacts, or a ripple visible by eye on the disc (Figure 1).

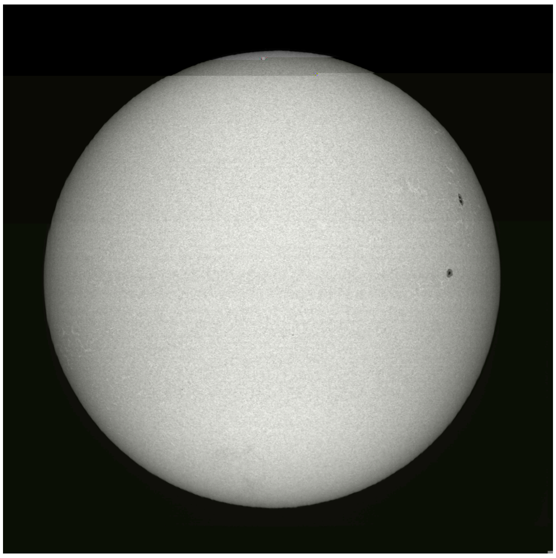

Figure 1: Example of an image reconstructed by JSol'Ex: the solar disc in the iron line, scan of 15 September 2026 at 10:04 UTC. The visual inspection was carried out on images of this kind. The analysed area is the central square, 830 pixels on a side.

Table 2: Observations of 15 September 2026.

Quantity	Value
Scans	336 retained out of 354 recorded
Volume of the retained scans	1.37 TB
Duration	6 h
Interval between scans	58.4 s before the meridian flip, 66.1 s after
Exposure	0.41 to 0.55 ms, adjusted between scans for a constant signal level
Analogue gain	100
Region of interest	3,088 × 128 px, 16 bits, at 322.6 frames/s
Solar elevation	20° to 46°
Seeing	judged poor

The mount was flipped at the meridian between 12:15 and 12:22 UTC. This flip mirrors the image about one axis; JSol'Ex compensates for it during reconstruction.

3 Data processing

3.1 Processing carried out in JSol'Ex

Everything is done in JSol'Ex 5.5.0, in a single batch process. Version 5.5.0 is a development version, not yet released at the time of the analysis; the author of this article is the developer of the software. The reference cited is therefore 5.4.2 [11], the latest archived version. The source code is public and 5.5.0 will be archived upon release. For each scan, the software locates the line in the video, reconstructs the images of the disc, fits the outline of the Sun with an ellipse, corrects the tilt and the difference in scale between the two axes of the image, and applies the flip. The analysis itself is a Python script run by the interpreter built into JSol'Ex: it receives the reconstructed images and their acquisition information, then computes the velocities, the diagram and the figures. The scientific analysis requires no other software: reconstructing the images, measuring the velocities and producing the diagram are all done within JSol'Ex. This is what makes it accessible to an amateur.

Acquisition was performed on a mini PC running Windows, with SharpCap and an automatic acquisition script in Python. As that machine is not particularly powerful, the files were processed on a separate computer. Processing the 354 files, including the computation of the diagram, took 2 h 30 on a computer with an AMD Ryzen 9 9950X processor (16 cores, 32 threads) and 128 GB of memory, running Linux Mint 22.3, the files being read from an external SSD connected over USB.

3.2 Images and analysed area

For each scan, JSol'Ex reconstructs not one but nine images, taken at nine neighbouring positions in the line: four on one side of the line centre, the centre itself, and four on the other side. These nine images give, at every point of the disc, the shape of the line.

The analysis covers an 830 × 830 pixel square centred on the disc, that is 417,000 km on a side. This conversion to kilometres uses the scale at disc centre; it is an approximation, acceptable here because the area stays close to the centre, where the surface is seen face-on. This choice follows the work of Gizon and Birch [8], who show that an area centred on the disc is enough to obtain a good diagram.

Over six hours, the rotation of the Sun moves the surface far enough that it must be taken into account: otherwise, different regions would be compared from one scan to the next. As the granulation is not resolved and the centre of the disc shows no stable detail, the area cannot be aligned on the images themselves. It is therefore tracked by computation: JSol'Ex provides the position of the disc in each image, and the displacement due to rotation is computed with the law of Snodgrass and Ulrich [12].

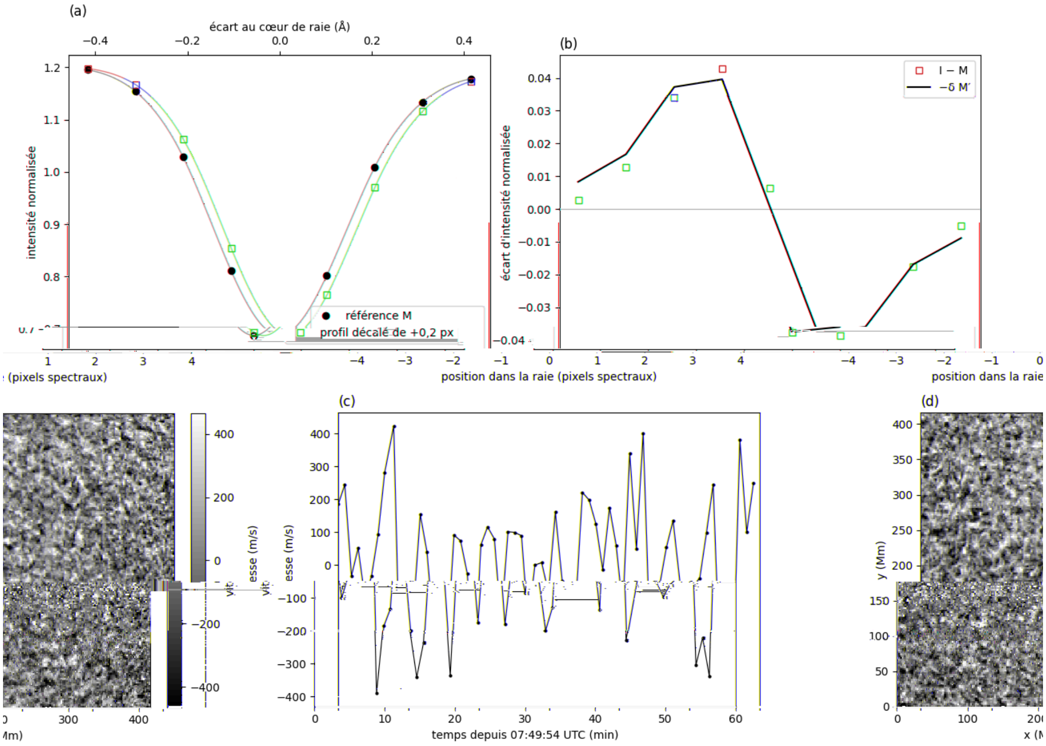

Figure 2: Doppler velocity measurement, 15 September 2026. (a) Mean shape of the line and the same shape slightly shifted. (b) Difference between the two, which is used to measure the shift. (c) Mean velocity of a small square at the centre of the area during the first hour: the five-minute oscillation can be seen directly. (d) Velocity map of one scan.

3.3 Measuring the velocities

The principle is to compare, at each point, the shape of the line observed at a given moment with its mean shape over the whole session (Figure 2).

The shape of the line. The nine images give nine brightness measurements that trace the dip of the line. They are divided by their mean, which removes brightness variations due to sky transparency, exposure time or the darkening of the disc towards its edge. Only the shape remains.

The reference. For each point of the disc, the mean shape of the line over the 336 scans is computed. This mean contains everything that does not change during the session, such as the defects specific to that point of the image. By comparing each measurement with the reference of the same point, these defects cancel out by themselves, without having to be modelled.

The shift. A motion of the surface shifts the line in wavelength. This shift is very small: a velocity of 300 m/s moves the line by only one twentieth of a pixel. It therefore cannot be read directly, but it can be deduced from the difference between the observed line and the reference line. This difference is proportional to the shift being sought, and its measurement uses all nine points at once, which makes it much more precise than a single pixel (Figure 2 b). The shift is then converted into a velocity.

There remain the slow drifts, which do not come from the Sun. For each scan, the median value of the whole image is removed, which eliminates anything affecting the whole image at once. For each point, its mean value and a straight line fitted by least squares over the six hours are then removed. Removing a single straight line over the whole series only affects variations slower than one oscillation per session, far below the frequencies studied here. The measurement noise is 212 m/s for one pixel and one scan; it is estimated from the scatter from one scan to the next, that is the standard deviation of the difference between two consecutive velocity maps, scaled to a single map. Averaging over 5 × 5 pixel squares, it drops to 42 m/s, whereas the measured velocity still varies by 166 m/s, nearly four times the noise: the variation is therefore clearly detectable in these data (Figure 2 c). Its solar origin, however, cannot be deduced from this comparison alone; it rests on the results that follow.

3.4 From the velocity cube to the diagram

At this stage, we have 336 velocity maps, one per scan: a film of the surface, taken every minute for six hours. These motions now have to be sorted by size and by rhythm.

Sorting by size is done on each map separately. It is a decomposition into ripples: we look for how much of the motion takes the form of large ripples, and how much takes the form of small ones. The calculation used is the Fourier transform, a standard tool that breaks an image down into ripples of different sizes and orientations.

Sorting by rhythm comes next, by following each ripple size from one scan to the next. A difficulty arises here: the scans are not evenly spaced in time, and the interval even changes during the session. Rather than forcing them onto a regular schedule, which would amount to giving them a false time, each scan is used at the exact time it

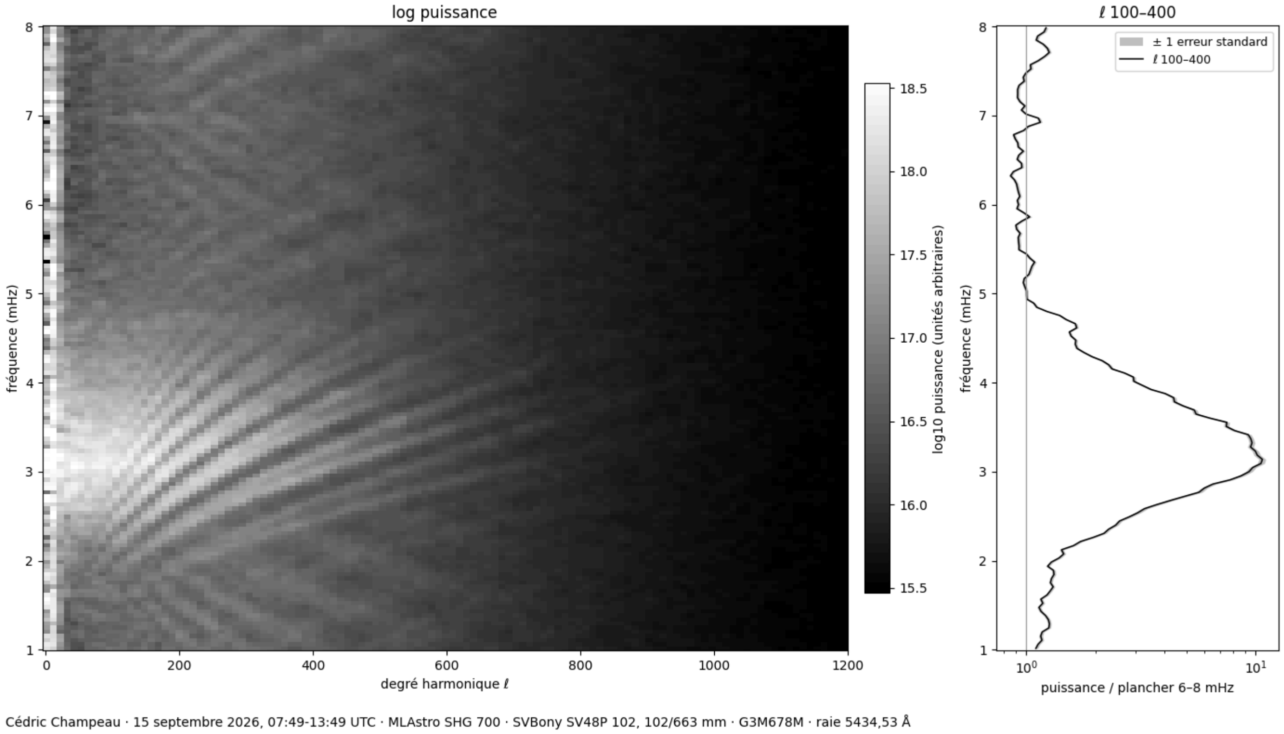

Figure 3: The diagram: the power of the motions as a function of degree, on the horizontal axis, and frequency, on the vertical axis. The brighter an area, the stronger the corresponding motion. On the right, the mean power for degrees 100 to 400, with its uncertainty.

was taken. Scans at the beginning and end of the session count slightly less than those in the middle, which avoids creating artefacts at the ends of the series, and each one is weighted according to the duration it represents.

The result is the diagram we are looking for: for each ripple size and each rhythm, the power of the corresponding motion. In practice, each scan is projected onto sine waves of increasing frequency, evaluated at its actual time and given its weight: this is a weighted Fourier transform, computed at the observation times rather than on a regular grid. The frequencies examined are multiples of the inverse of the session duration, that is multiples of 46 microhertz: this is the frequency resolution of the series. At the other end, the interval of about one minute between scans sets the highest accessible frequency, known as the Nyquist frequency: 8.6 millihertz before the meridian flip, 7.6 after. The background level, which we measure between 6 and 8 millihertz, comes close to it, which calls for caution near 8. Finally, since the waves travel in all directions, the powers are averaged over all orientations of the same ripple size. The uncertainty given for each point of the diagram is the standard error of this mean, that is the standard deviation of the averaged values divided by the square root of their number. It is a statistical uncertainty on the mean power, not an overall accuracy of the measurement.

4 Results

The figures and values in this section come from the processing described above, with no further correction. Section 5 presents the gain obtained by correcting the mount's tracking defect.

4.1 The diagram

Figure 3 shows the diagram obtained, and Figure 4 the same diagram with reference marks added.

The diagram clearly shows what Ulrich predicted: the power is not distributed at random, but concentrated along lines. It peaks at 3.14 mHz, that is one oscillation every 5 minutes and 18 seconds. Between 2.5 and 4 mHz, it is nearly seven times stronger than the background level measured between 6 and 8 mHz.

Above 5 mHz, the power drops and reaches a floor around 5.5 mHz. This value is of the order of the acoustic cut-off frequency of the photosphere: beyond it, the waves propagate more readily into the upper layers instead of remaining confined in the cavity where they resonate.

4.2 The ridges compared with space measurements

Separate ridges are visible from degree 100 to about degree 800. The frequency of each ridge is not simply read at the position of the maximum: a curve is fitted to the five points surrounding that maximum, which locates the peak more finely than a single point of the spectrum and provides its uncertainty. These values are compared with the ridges of a published diagram from the SOHO satellite (Table 3). The uncertainty given concerns only our measurement; reading the SOHO ridges from a published figure has its own imprecision, of a few tens of microhertz.

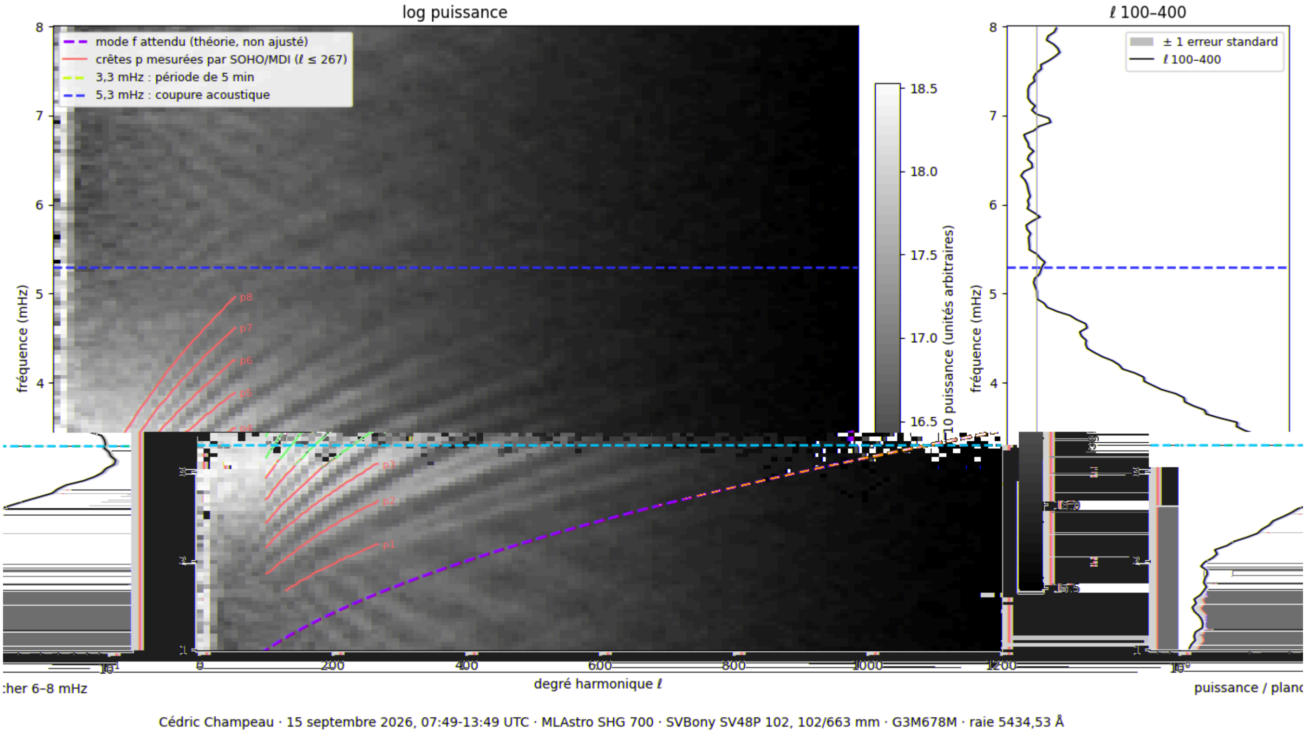

Figure 4: Same diagram with reference marks. In orange, the theoretical position of the f mode, computed without any adjustment from the surface gravity wave relation given by Gizon and Birch [8], with the gravity at the Sun's surface and its radius as the only constants. In green, the ridges read from a published diagram from the SOHO satellite [13], built from the measurements of MDI's medium-ℓ programme [14]. The straight lines mark 3.3 and 5.3 mHz.

Table 3: Frequencies of the six ridges, in millihertz, with their uncertainty, compared with the values read from the SOHO diagram.

Ridge	Degree 199	SOHO	Degree 252	SOHO
p1	1.916 ± 0.044	1.96	2.094 ± 0.008	2.14
p2	2.381 ± 0.009	2.39	2.604 ± 0.010	2.61
p3	2.763 ± 0.003	2.77	3.016 ± 0.008	3.03
p4	3.131 ± 0.004	3.14	3.392 ± 0.009	3.41
p5	3.458 ± 0.004	3.47	3.786 ± 0.006	3.79
p6	3.800 ± 0.007	3.79	4.139 ± 0.051	4.16

This agreement is the most robust result of this work. The differences range from −0.046 to +0.010 mHz: ten of the twelve ridges fall within 21 microhertz of the SOHO value, less than half a resolution element. The two largest differences, p1 at degree 199 and p6 at degree 252, are also those whose peak is least sharp, with uncertainties of 44 and 51 microhertz. The agreement relies on no tuning at all: the frequency scale comes solely from the time stamps of the files, and the size scale solely from the disc radius measured in pixels. Two shorter sessions, on 13 and 14 September, show the same ridges, with lower precision owing to their shorter duration.

4.3 Comparison with published frequencies

The previous comparison relies on reading a figure. The MDI project also publishes its frequencies as lists of numbers, fitted directly to its spectra [15]. Unfortunately, these lists do not extend far enough towards small waves to cover degrees 199 and 252: at degree 199 they contain only the first ridge, and at degree 252 none at all. The comparison is therefore repeated at degree 126, where all six ridges are tabulated (Table 4).

Table 4: Our six ridges at degree 126, compared with the frequencies published by MDI. Frequencies are in millihertz, differences in microhertz.

Ridge	Published value	Our measurement	Difference
p1	1.6441 ± 0.0003	1.659 ± 0.004	+15
p2	2.0072 ± 0.0008	2.027 ± 0.005	+20
p3	2.3404 ± 0.0014	2.347 ± 0.005	+7
p4	2.6356 ± 0.0024	2.635 ± 0.004	−1
p5	2.9201 ± 0.0038	2.927 ± 0.009	+6
p6	3.1902 ± 0.0041	3.175 ± 0.010	−15

The mean difference is 11 microhertz, a quarter of the resolution of our series. The same comparison gives 16 at degree 147 and 25 at degree 168. At degree 105, however, our frequencies are systematically too high, by 41 on average.

4.4 The smallest waves fade away

Figure 5 compares the power of the oscillations for four ranges of size.

Table 5: The contrast of the oscillations drops as the waves get smaller.

Degree range	Power of the oscillations, relative to the background
30–100	28.0 ± 0.4
100–200	13.8 ± 0.1
200–400	4.79 ± 0.04
400–600	1.90 ± 0.01

The power of the oscillations, relative to the background, is about fifteen times weaker for degrees 400 to 600 than

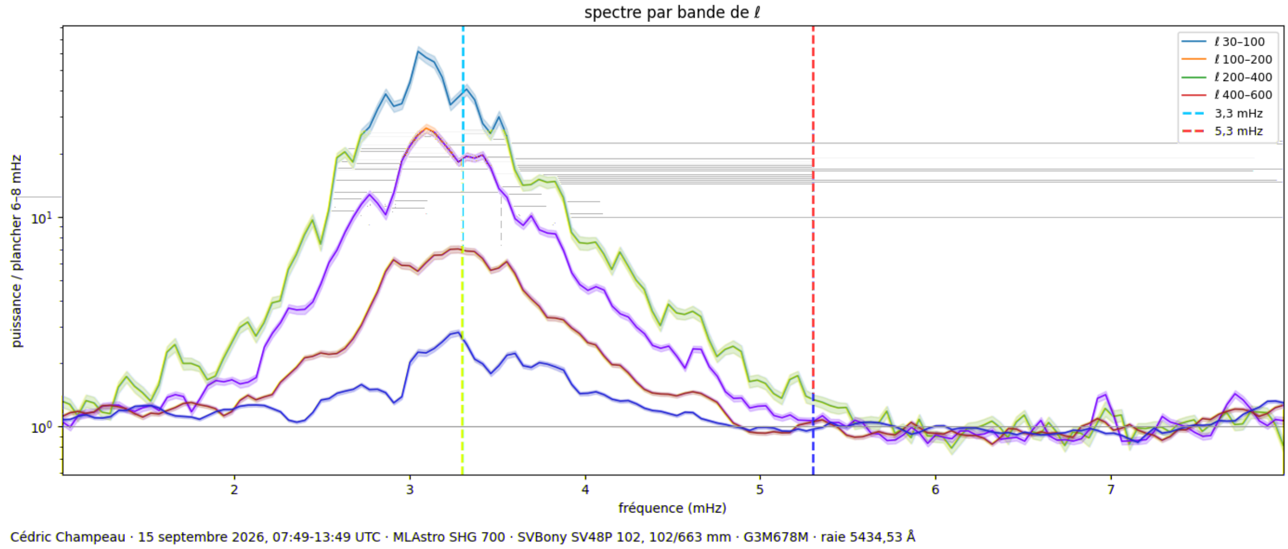

Figure 5: Mean power as a function of frequency, for four ranges of degree. The shaded areas represent the uncertainty.

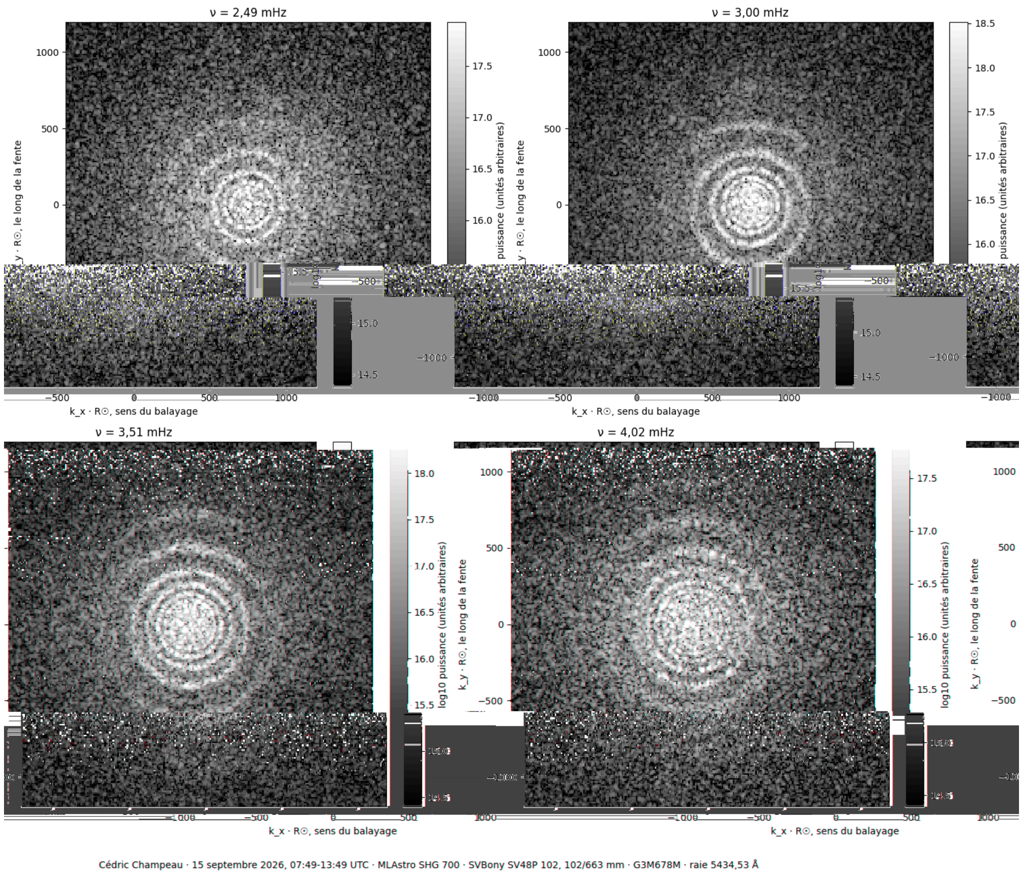

Figure 6: View of the diagram at four fixed frequencies. Each image shows the power according to the direction and size of the waves; the centre corresponds to the largest ripples. The horizontal axis is the scan direction, the vertical axis that of the slit.

cannot separate them: turbulence in the Earth's atmosphere, which blurs the finest details, and the resolving power of the instrument, which attenuates them. This is the main limitation of an observation made from the ground, and it explains why degree 800 is the practical detection limit for the ridges here.

4.5 Rings rather than ridges

If we choose one frequency and look at all directions at once, each ridge becomes a ring (Figure 6). The radius of the ring gives the size of the waves, and the concentric rings correspond to the successive families. They are sharp between 2.5 and 3.5 mHz, and more diffuse at 4 mHz.

4.6 The f mode

There is another family of waves, called the f mode. These are not sound waves but surface waves, comparable to waves on water. Their theoretical position is plotted in orange in Figure 4; no ridge follows it. A band of power is nevertheless visible just below it, from degree 250 to degree 900: it is examined in Section 6.

5 An imperfection of the mount, measured and corrected

5.1 The origin of the problem

The mount drives the telescope to compensate for the rotation of the Earth, but it does so with a small irregularity that repeats every 430 seconds, with an amplitude of about 16 arcseconds. The manufacturer confirmed this period and amplitude.

While a scan is being recorded, this irregularity slightly changes the speed at which the image of the Sun drifts across the slit. JSol'Ex corrects the mean scale of each scan and recentres the disc, but a distortion remains that shifts the content of the image by a few pixels, differently from one scan to the next. Successive velocity maps therefore end up slightly offset from one another, which blurs the ridges.

5.2 The correction

It is applied to the velocity maps already computed, without reprocessing the videos, and takes a few minutes. It proceeds in three steps.

1. **Measure.** Each velocity map is compared with the previous one to determine how far its content has slipped. The measurement is made in four strips spread along the scan, since the slip is not the same everywhere. Velocity maps are well suited to this measurement because they are rich in detail, unlike ordinary images of the disc.
2. **Model.** From these measurements, only what repeats at the mount's own rhythms is kept: 431.6 seconds and two faster rhythms derived from it. Everything else is ignored, which avoids correcting anything other than the mount. The model accounts for 29 to 73 % of the observed slip depending on the strip, and the slip reconstructed in this way reaches 6 pixels before the meridian flip, and 13 pixels after (Figure 7 a).
3. **Correct.** Each velocity map is put back in place according to this model, and the diagram is recomputed.

To make sure that the gain really comes from the mount and not from chance, the same correction was applied to randomly drawn scans. If the method improved things merely by construction, this control would improve as well.

5.3 The result

Table 6: Effect of the correction, compared with the randomly drawn control.

Measure	Before	After	Control
Power along the SOHO ridges, relative to the background	0.234	0.258	0.211
Sharpness of the ridges, degrees 200 to 600	11.7	13.7	9.8
Sharpness of the ridges, degrees 600 to 800	2.9	3.2	2.3
Power of the oscillations, degrees 100 to 400	6.8	9.9	5.5

The correction improves every measure, whereas the randomly drawn control degrades them (Table 6). This result is consistent with a gain due to correcting the periodic motion of the mount. It mainly affects the waves travelling along the scan direction, which is precisely the direction in which the mount acts. On the diagram, oblique patterns with no physical meaning fade away (Figure 7 b and c).

The contrast of the oscillations increases by half (Table 7), while the frequencies of the ridges move by no more than the frequency resolution: the correction makes the diagram sharper without displacing what it contains. Their agreement with SOHO even improves, the largest difference falling from 46 to 24 microhertz.

6 A band close to the f mode

Figure 8 enlarges the region of the f mode. A band of power is clearly visible there from degree 250 to degree 900. Its slope is close to that of the theoretical f-mode curve, but it is systematically shifted towards lower frequencies: 4 % lower near degree 300, and 8 % lower near degree 900. It is present both before and after the correction of the mount, and is also found in the sessions of 13 and 14 September.

This band does not match the f mode as it is measured. The frequencies published by MDI [15] extend up to degree 300: the f mode lies there 0.7 to 1.2 % *above* the theoretical curve, about a dozen microhertz, and never below. Further out, it stays within a few microhertz of theory up to degree 700, and falls 13 microhertz below at degree 880 [16]. Our band, by contrast, is more than ten times lower. Variations of the f mode over the solar activity cycle do not explain it either: they amount to a few hundredths of a microhertz, a change in the radius of the Sun of about 5 km [17], far from the tens of microhertz measured here.

This difference is not the same everywhere, however. Near degree 300, it is 69 microhertz, barely more than the width of the band itself: at that point, the band remains compatible with the f mode. Near degree 750, it reaches 195 microhertz, four times the frequency resolution, and the difference becomes clear. The nature of this band therefore remains to be established.

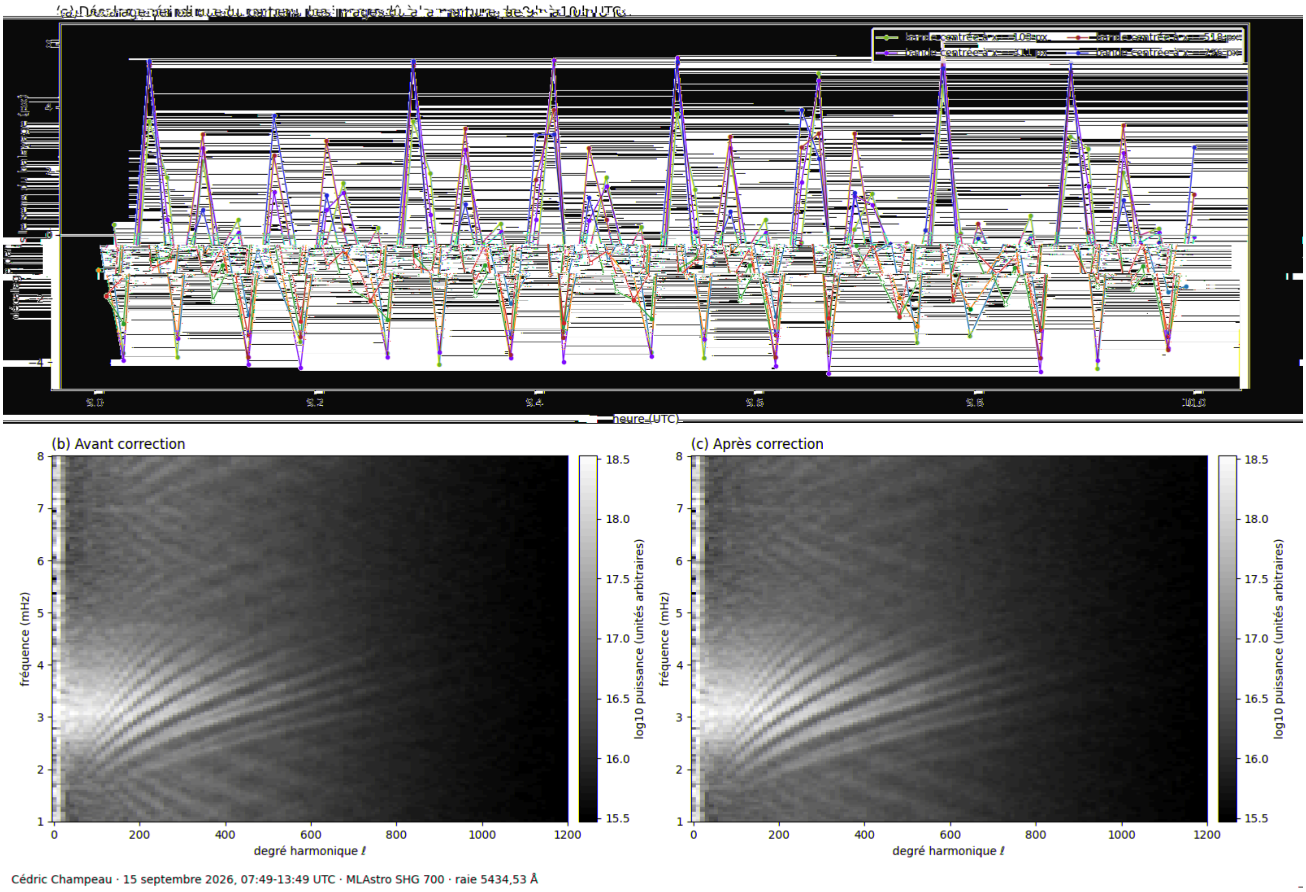

Figure 7: Correction of the mount's irregularity. (a) Reconstructed slip of the image content, for the four strips, between 9 and 10 h UTC. (b) Diagram before correction. (c) After correction, with the same grey scale.

Table 7: The same measures before and after correction.

Measure	Without correction	After correction
Frequency of the maximum	3.14 ± 0.05 mHz	3.14 ± 0.05 mHz
Power of the oscillations, degrees 100 to 400	6.79 ± 0.04	9.86 ± 0.06
Power just below the trapping limit	1.87 ± 0.01	2.34 ± 0.01
Contrast, degrees 30 to 100	28.0 ± 0.4	33.3 ± 0.5
Contrast, degrees 100 to 200	13.8 ± 0.1	19.5 ± 0.2
Contrast, degrees 200 to 400	4.79 ± 0.04	7.21 ± 0.05
Contrast, degrees 400 to 600	1.90 ± 0.01	2.62 ± 0.01
Difference of the ridges from the SOHO values	−0.046 to +0.010 mHz	−0.024 to +0.007 mHz

7 Discussion

7.1 Comparison with ground-based observations

Deubner [3] could distinguish three or four ridges from the ground; the diagram presented here separates six of them, and allows them to be identified by comparison with SOHO.

That the f mode does not clearly appear is not surprising. Gizon and Birch [8] compare two diagrams obtained at the same time, one from space with SOHO, the other from the ground with the TON network, in conditions close to those of this work: the f-mode ridge is markedly weaker as seen from the ground. With a 102 mm refractor and a poor sky, its absence is consistent with what published ground-based observations show.

7.2 Limitations

- **Atmospheric turbulence.** The f mode stands out mostly among small waves, which is precisely where turbulence erases the most power.
- **The correction of the mount.** It only deals with the slip along the scan direction, with three rhythms and four strips. The slip is measured on the very data that are then corrected; the control shows that the gain does come from the mount, but it cannot be ruled out that a small share of solar signal at the same rhythms was affected.
- **The reference values at degrees 199 and 252.** They were read from a published figure, for lack of frequency lists covering these degrees: the position of the ridges is located on the image and converted using the axis graduations. The accuracy of such a reading is of the same order as the measured differences, so it is not possible to

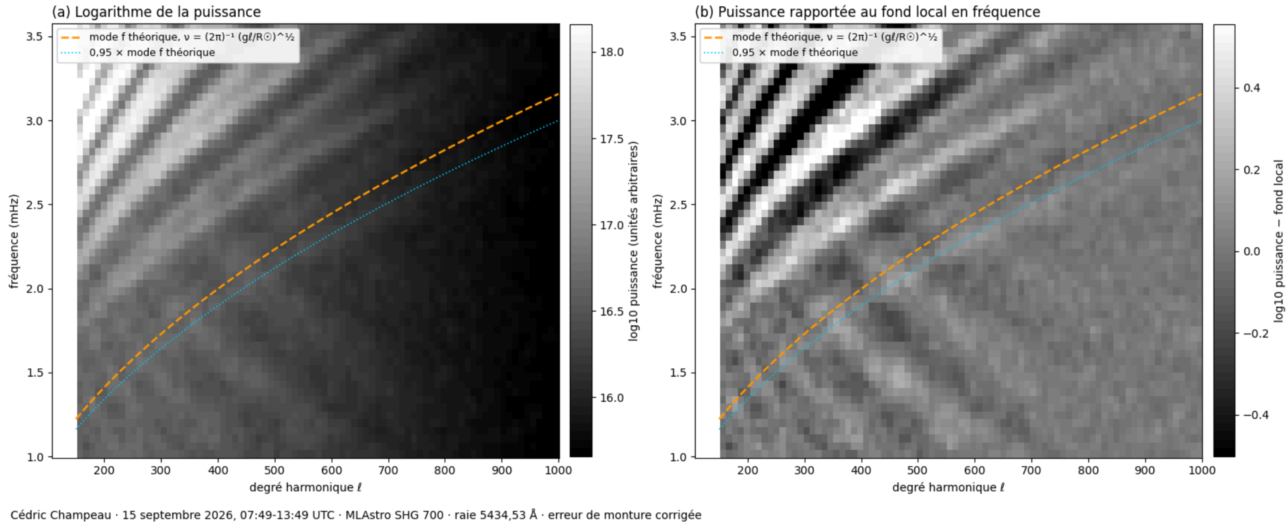

Figure 8: The f-mode region, after correction of the mount. (a) The power as it is. (b) The same power after subtracting the background, which brings out the fine structures. In orange, the theoretical position of the f mode according to Gizon and Birch [8]; in cyan, the same curve lowered by 5 %.

tell what comes from the Sun, from the instrument, or from the reading. Comparison with the published lists is only possible at degree 168 and below.

- **A single session.** The available sessions have not been combined.

8 Conclusions and outlook

We have not identified any publication presenting an equivalent measurement made by an amateur, after searching bibliographic databases, preprint archives, and the websites and forums of the amateur spectroheliograph community: the Sun's five-minute oscillations are detected here with an amateur spectroheliograph, and their families of waves separated one by one. Six ridges are resolved up to degree 800, and their frequencies are compatible, within the accuracy allowed by reading the published figure, with those of the SOHO diagram. JSol'Ex's batch processing and its Python interpreter make this measurement accessible.

A doubt remains about the f mode: a band is visible near its expected position, but it does not match the published frequencies.

Several avenues remain open: integrating the mount correction into JSol'Ex processing, combining several sessions to gain precision, and extending the comparison with published tables towards high degrees. Beyond degree 190, the reference frequencies are no longer given by the observatories' usual tables, but by specialised analyses.

9 Acknowledgements and AI use statement

This article was written with the assistance of the artificial intelligence Claude (Anthropic). The measurement protocol and the processing pipeline were designed by the author from the scientific literature. The software implementation of that pipeline was carried out in cooperation with the AI: it produced the Python code, while the author directed its design, identified numerous errors and had them corrected, and validated the final version. Likewise, the analysis of the results was written with the assistance of the AI, which proposed interpretations and comparisons with the literature. The author reviewed and validated the final text.

Thanks to Minh Nguyen, of MLAstro, for identifying the periodic error of the mount and for measuring its amplitude.

References

[1] R. B. Leighton, R. W. Noyes, and G. W. Simon, "Velocity Fields in the Solar Atmosphere. I. Preliminary Report," *The Astrophysical Journal*, vol. 135, p. 474, 1962, doi: 10.1086/147285.

[2] R. K. Ulrich, "The Five-Minute Oscillations on the Solar Surface," *The Astrophysical Journal*, vol. 162, p. 993, 1970, doi: 10.1086/150731.

[3] F.-L. Deubner, "Observations of low wavenumber nonradial eigenmodes of the Sun," *Astronomy and Astrophysics*, vol. 44, p. 371, 1975.

[4] J. Christensen-Dalsgaard, "Helioseismology," *Reviews of Modern Physics*, vol. 74, p. 1073, 2002, doi: 10.1103/RevModPhys.74.1073.

[5] T. Sekii *et al.*, "Initial Helioseismic Observations by Hinode/SOT," *Publications of the Astronomical Society of Japan*, vol. 59, p. S637, 2007, doi: 10.1093/pasj/59.sp3.s637.

[6] J. Christensen-Dalsgaard, *Lecture Notes on Stellar Oscillations*, 5th ed. Aarhus Universitet, 2014.

[7] J.-M. Malherbe, F. Cornu, and I. Bualé, "Solex observations for the BASS2000 database, a collaboration PRO-AM," 2023. [Online]. Available: https://arxiv.org/abs/2305.14804

[8] L. Gizon and A. C. Birch, "Local Helioseismology," *Living Reviews in Solar Physics*, vol. 2, p. 6, 2005, doi: 10.12942/lrsp-2005-6.

[9] I. I. Yakovkin and V. G. Lozitsky, “Strong Zeeman effects in the Fe I 5434.5 Å line observed in a sunspot on August 17, 2024,” 2026. [Online]. Available: https://arxiv.org/abs/2608.06316

[10] N. Bello González, M. Flores Soriano, F. Kneer, O. Okunev, and N. Shchukina, “Acoustic waves in the solar atmosphere at high spatial resolution. II. Measurement in the Fe I 5434 Å line,” *Astronomy & Astrophysics*, vol. 522, p. A31, 2010, doi: 10.1051/0004-6361/201014052.

[11] C. Champeau, “JSol'Ex, version 5.4.2 archived on Zenodo.” Zenodo, 2026. doi: 10.5281/zenodo.22666115.

[12] H. B. Snodgrass and R. K. Ulrich, “Rotation of Doppler features in the solar photosphere,” *The Astrophysical Journal*, vol. 351, p. 309, 1990, doi: 10.1086/168467.

[13] Wikimedia Commons, “MDI medium angular degree power spectrum.” [Online]. Available: https://commons.wikimedia.org/wiki/File:MDI_medium_angular_degree_power_spectrum.png

[14] E. J. Rhodes Jr., A. G. Kosovichev, J. Schou, P. H. Scherrer, and J. Reiter, “Measurements of Frequencies of Solar Oscillations from the MDI Medium-l Program,” *Solar Physics*, vol. 175, pp. 287–310, 1997, doi: 10.1023/a:1004963425123.

[15] Solar Oscillations Investigation (JSOC/Stanford University), “Solar mode frequencies, series mdi.vw_V_sht_modes of the SOHO/MDI medium-l programme.” [Online]. Available: http://jsoc.stanford.edu/MDI/MDI_Global.html

[16] M. C. Rabello-Soares, S. G. Korzennik, and J. Schou, “Analysis of MDI High-Degree Mode Frequencies and their Rotational Splittings,” *Solar Physics*, vol. 251, pp. 197–224, 2008, doi: 10.1007/s11207-008-9231-7.

[17] H. M. Antia, S. Basu, J. Pintar, and B. Pohl, “Solar Cycle Variation in Solar f-Mode Frequencies and Radius,” *Solar Physics*, vol. 192, pp. 459–468, 2000, doi: 10.1023/a:1005204800696.